inorganics MDPI

Article

N-O ligand Supported Stannylenes: Preparation, Crystal, and Molecular Structures.

Hannah S. I. Sullivan [1,2], Andrew J. Straiton [1] Gabriele Kociok-Köhn [3] and Andrew L. Johnson [1,*]

[1] Department of Chemistry, University of Bath, Bath. BA2 7AY. United Kingdom
[2] Centre for Sustainable Chemical Technologies, University of Bath, Bath. BA2 7AY, United Kingdom.
[3] Material and Chemical Characterisation Facility (MC[2]), University of Bath. BA2 7AY, United Kingdom.

* Correspondence: a.l.johnson@bath.ac.uk

Abstract: A new series of tin(II) complexes (**1**, **2**, **4** and **5**) were successfully synthesized by employing hydroxy functionalized pyridine ligands, specifically 2-hydroxypyridine (hpH), 8-hydroxyquinoline (hqH) and 10-hydroxybenzo[h]quinoline (hbqH) as stabilizing ligands. Complexes $[Sn(\mu\text{-}\kappa^2ON\text{-}OC_5H_4N)(N\{SiMe_3\}_2)]_2$ (**1**) and $[Sn_4(\mu\text{-}\kappa^2ON\text{-}OC_5H_4N)_6(\kappa^1O\text{-}OC_5H_4N)_2]$ (**2**) are the first structurally characterized examples of tin(II) oxypyridinato complexes exhibiting $\{Sn_2(OCN)_2\}$ heterocyclic cores. As part of our study ^{1}H DOSY NMR experiments were undertaken, using an external calibration curve (ECC) approach, with temperature independent normalized diffusion coefficients, to determine the nature of oligomerisation of **2** in solution. An experimentally determined diffusion coefficient (298K) of 6.87 x10^{-10} m^2 s^{-1}corresponds to a hydrodynamic radius of *Ca.* 4.95 Å. This is consistent with the observation of an averaged hydrodynamic radii, and equilibria between dimeric $[Sn\{hp\}_2]_2$ and tetrameric $[Sn\{hp\}_2]_4$ species at 298K. Testing this hypothesis ^{1}H DOSY NMR experiments were undertaken at regular intervals between 298K-348K and shows a clear change in the calculated hydrodynamic radii form 4.95Å (298K) to 4.35Å (348K) consistent with a tetramer ⇄ dimer equilibria which lies towards the dimeric species at higher temperatures. Using these data, thermodynamic parameters for the equilibrium ($\Delta H°$ = 70.4(±9.22) kJ mol^{-1}, $\Delta S°$ = 259(±29.5) J K^{-1} mol^{-1} and $\Delta G°_{298}$= -6.97 (±12.7) kJ mol^{-1}) were calculated. In the course of our studies the Sn(II) oxo cluster, $[Sn_6(m^3\text{-}O)_6(OR)_4{:}\{Sn^{(II)}(OR)_2\}_2]$ (**3**) (R = C_5H_4N) was serendipitously isolated and its molecular structure determined by single crystal X-ray diffraction analysis. However, attempts to characterise the complex by multinuclear NMR spectroscopy was thwarted by solubility issues and attempts to synthesise **3** on a larger scale, were unsuccessful. In contrast to the oligomeric structures observed for **1** and **2**, single crystal X-ray diffraction studies unambiguously establish the ~~monomentic~~ monomeric 4-coordinate solid state structures of $[Sn(\kappa^2ON\text{-}OC_9H_6N)_2)]$ (**4**) and $[Sn(\kappa^2ON\text{-}OC_{13}H_8N)_2)]$ (**5**).

Keywords: Stannylene; 2-hydroxy-pyridine; 8-hydroxyquinoline; 10-hydroxybenzo[h]quinoline; molecular structures, DOSY NMR.

Citation: Lastname, F.; Lastname, F.; Lastname, F. Title. *Inorganics* **2022**, *10*, x. https://doi.org/10.3390/xxxxx

Academic Editor: Firstname Lastname

Received: date
Accepted: date
Published: date

Formatted: Font: Bold

Formatted: Font: Bold

1. Introduction

The chemistry of heavy carbene analogues [MR_2 : M = Si, Ge, Sn, Pb; R = stabilizing anionic ligand) has attracted considerable interest for some time now and is of fundamental interest in main group p-block chemistry[1-3] Their marked dual Lewis acidic and

Lewis basic characteristics, alongside steric and electronic tuneability via astute ligand selection, results in a diverse and often unique chemistry.[2]

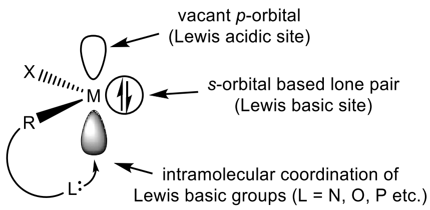

Figure 1. Stabilization of stannylene [Sn(R-L)$_{2-x}$(X)$_x$)] complexes.

A particular class of tetrylenes of interest are the stannylene complexes with general formula [Sn(R-L)$_{2-x}$(X)$_x$], where [R-L] is a monoanionic ligand bearing a lariat donor group (L) fragment capable of forming either intra- or inter-molecular Lewis base adducts with the metal atom, Figure 1, thus acting as an anionic chelate or bridging ligand, and where X is an ancillary monodentate ligand such as a halogen atom or {N(SiMe$_3$)$_2$} group.[4-9] These Sn(II) compounds have potential application as ligands for transition metals, intermediates in organic synthesis,[10-13] catalysts in the conversion of small molecules[14-20] or the ring opening polymerisation of lactones,[21] or as precursors for electronic thin film materials.[8,18,22-26]

It is well established that the nature of the ligand (donor atoms) has a significant effect on the chemical and structural properties of these heavy carbene analogues. Amongst the library of [Sn(II)(R-L)$_{2-x}$(X)$_x$] systems, perhaps the most frequently studied are those bearing an N-N′ chelate as the [R-L] ligands, such as amidinates,[22,27-29] guanidinates,[8,25,30-33] β-diketiminates[5,21,34-39] and amino/imino-pyrrolides.[9] While Sn(II) [Sn(R-L)$_{2-x}$(X)$_x$] systems bearing an *N,O* chelate ligand such as amino alcohols,[7,40-48] amino-phenols,[49] organic amides,[23,50] salicylaldiminato,[50-53] ketiminate[54] and hydroxyquinolinates,[55-64] are known, their derivative chemistry is less developed.

While the anionic derivatives of 2-hydroxypyridine (hpH) [65,66] and 8-hydroxyquinoline (hqH)[67,68] have been utilized as 1,3- 1,4-k^{2}N,O chelate ligands respectively for a range of metals, examples of the coordination chemistry of 10-hydroxybenzo[h]quinoline (hbqH) (Figure 2) and its derivatives are scarce, despite its commercial availability.
The anions of 2-hydroxypyridine derivatives belong to a wider class of tri-atomic bridging ligands, such as carboxylate, triazenide, amidinate, sulfonates and phosphates.[65,69] The presence of two different donor atoms results in a rich coordination chemistry with a variety of potential binding modes for the oxypyridinato ligand, common examples of which are shown in Figure 2, illustrating the unusual binding modes of the {hp} ligand that constrained 1,3-N,O (four-membered ring) coordination can induce. A search of the literature reveals numerous oxypyridinato ligated transition metal complexes, whilst there are in comparison only a handful of main group complexes (reported in the CSCD),[70-75] and to-date none of these represent Sn(II) supported species. In contrast, the quinolinato, {hq} and the oxybenzo[h]quinolinato {hbq} ligands exclusively display 1,4- and 1,5-κ^2-N,O coordination modes respectively.

To-date, Sn(II) derivatives of these systems (*i.e.* {hp}, {hq} and {hbq}), are limited to a handful of homoleptic[61,64] and heteroleptic[55-60,62,63] Sn(II) hydroxyquinolate complexes. Here we describe the details of the synthesis and structure of a series of Sn(II) complexes supported by the 1,3-, 1,4- and 1,5-κ²N,O chelate ligands oxypyridinato (hpH), hydroxyquinolinato {hqH} and oxybenzo[h]quinolinato {hbq} respectively.

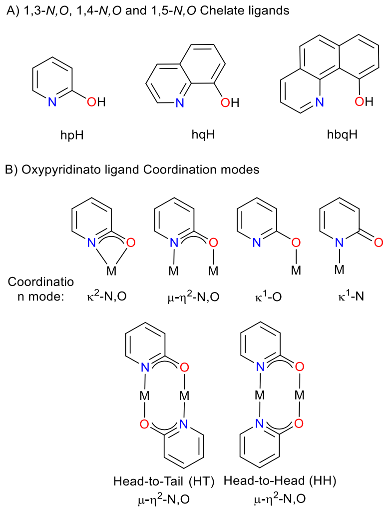

Figure 2. Overview of the *N,O* donor pro-ligands, hpH, hqH and hbqH used in this study (A), and the common coordination modes observed for the 2-hydroxpyridinato (hp) ligand (B).

2. Synthesis of Tin(II) Complexes: In all cases, isolated products were characterised by solution state NMR (^{1}H, ^{13}C{^{1}H} and ^{119}Sn{^{1}H}) spectroscopy and elemental analysis. Reaction of the bulky Sn(II) amide system [Sn{N(SiMe$_3$)$_2$}$_2$] with ligand 2-hydroxypyridine in a stoichiometric 1:1 reaction results in the formation and isolation after recrystallisation (-28 °C in toluene), of complex **1** as pale yellow crystals (Scheme 1). The ^{1}H NMR spectrum of **1** (in C_6D_6) clearly shows the presence of a singlet resonance at δ = 0.37 ppm representative of the presence of an {HMDS} group. The ^{1}H NMR spectra also clearly shows a series of four multiplets corresponding to the aromatic protons of the {hp} ligand at δ = 6.20, 6.48, 6.97 and 7.99 ppm respectively, in a 1:1:1:1:18 ratio with the {N(SiMe$_3$)$_2$} group, indicating the formation of a mono-substituted complex of the general form [{hp}Sn{N(SiMe$_3$)$_2$}]. This is supported by the ^{13}C{^{1}H} NMR spectra which clearly shows the expected six resonances [δ = 170.0, 142.6, 142.2, 116.6 114.0 and 5.9 ppm].

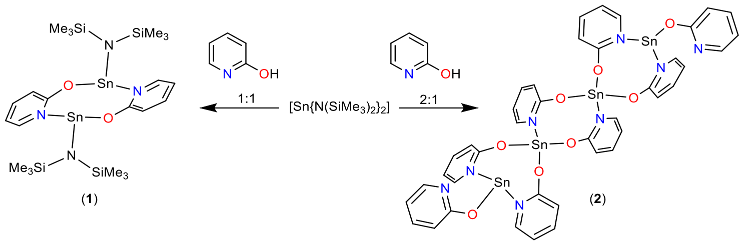

Scheme 1. Formation of complexes **1** and **2**.

Likewise, the ^{119}Sn{^{1}H} NMR spectra shows a single sharp resonance [δ = –84.9 ppm] respectively (*Cf.* δ = 776.0 ppm, for [Sn{N(SiMe$_3$)$_2$}$_2$]). Reaction of [Sn{N(SiMe$_3$)$_2$}$_2$] with 2 equivalents of 2-hydroxypyridine in toluene results in the formation of a colourless precipitate which after heating into solution followed by filtration and cooling afforded a crop of colourless crystals of **2**. The ^{1}H NMR spectrum of **2** (in C_6D_6) shows only four multiplets corresponding to the aromatic protons of the {hp} ligand at δ = 6.02, 6.62, 6.92 and 7.63 ppm respectively, in a 1:1:1:1 ratio. The clear absence of a peak corresponding to the {N(SiMe$_3$)$_2$} group indicates the formation of a *bis*-substituted complex of the general form [Sn{hp}$_2$]. The ^{13}C NMR spectra consists of ~~six~~ five resonances [δ = 112.7, 115.7, 140.4, 143.7 and 169.3 ppm], while the ^{119}Sn NMR spectra displays a single broad resonance at δ = –525.5 ppm. Low temperature NMR studies (~~-50~~223 ~~°C~~K) on complex **2**, in d$_8$-Tol, showed no ~~changes~~ significant changes in the ^{1}H, ^{13}C{^{1}H} or ^{119}Sn{^{1}H} NMR spectra, suggestive of a exchange process faster than the NMR time scale even at 223K. Below ~~-50 °C~~223K, low solubility issues resulted in ~~of in a~~ loss ~~if~~ of the ^{119}Sn signal.

To determine the nature of oligomerisation of **2** in solution ^{1}H DOSY NMR experiments were undertaken, using the novel external calibration curve (ECC) approach, with temperature independent normalized diffusion coefficients, for MW-determination described by Stalke et al.[76,77]

The room temperature (298K) ^{1}H DOSY NMR spectrum for compound **2**, shown in ~~Figure~~ Figure 3, clearly shows a single diffusion coefficient (D_{norm} = 6.87 x10^{-10} m^2 s^{-1}) which corresponds to a hydrodynamic radius of *Ca.* 4.95 Å.

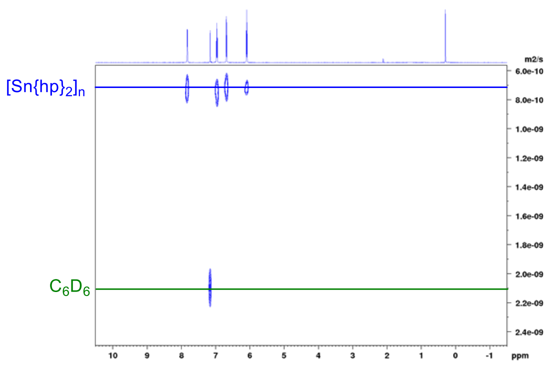

Figure 3. Plot showing the ^{1}H DOSY NMR spectrum for compound **2** (298K).

Commented [AJ1]: Change to Scheme has been made

Commented [AJ2]: Comment added here to explain the observation of only one set of sharp resonances in the 1H and 13C NMR spectra of compound 2, even at low temperature.

Formatted: Superscript

Based on the single crystal data (*infra vide*), the molecular volume of the tetrameric **2** observed in the solid state calculated as *ca*. 721 Å^3, with a molecular radius of 5.56Å. While molecular shapes are important to the accurate interpret diffusion data, diffusion coefficient/molecular weight corelation studies have shown that merged calibration curves based around molecules in solution behaving as either (i) compact spheres, (ii) dissipated spheres or ellipsoids and (iii) expanded discs can be used to estimate molecular weights.

Assuming each "[Sn{hp}$_2$]" unit is "spherical" and possesses an approximate volume of 183 Å^3, as determined by X-ray crystallography, the experimentally determined hydrodynamic volume, based on the Stokes-Einstein equation, is consistent with the presence of a trimeric species in solution. While a trimeric species is possible, we believe a more likely scenario is that the experimentally determined hydrodynamic volume is an averaged diffusion coefficient (and hydrodynamic volume) constant with a rapid (on the NMR timescale) equilibria between dimeric [Sn{hp}$_2$]$_2$ and tetrameric [Sn{hp}$_2$]$_4$ species (Scheme 2) at 296K.

Using Stalke's method, and correcting empirically for molecular density (using an empirically determined density correction factor of 1.5535 and hence accounting for the heavy Sn atom),[78] we predict a molecular mass of 937 Da (*c.f.* a calculated mass for a trimeric species [Sn{hp}$_2$]$_3$ of 921 Da, 2% error). To test our hypothesis ^{1}H DOSY NMR experiments were undertaken at regular intervals between 298K-348K. Table 1 and F~~f~~igure ~~3~~4, show the diffusion coefficients of **2**, 5.43mM in d8-Tol as a function of temperature. At 298K ^{1}H DOSY NMR affords an experimentally determined diffusion coefficient of D = 7.97x10^{-10} m^2 s^{-1}, which on warming to 348 K increases to D = 1.75x10^{-9} m^2 s^{-1}. The observed change in the calculated hydrodynamic radii is concomitant with a decrease in the calculated hydrodynamic radii, such that at 348K $R_{Hyd\text{-}cal}$ = 4.37 Å (*cf.* $R_{Hyd\text{-}cal}$ = 4.93 Å at 298K and a crystal graphically determined R = 4.44Å) consistent with a tetramer ⇄ dimer equilibria which lies towards the dimeric species at higher temperatures. When cooled to room temperature, the observed diffusion coefficient returns to D = 7.97x10^{-10} m^2 s^{-1}, implying a low barrier to tetramer formation.

A subsequent attempt was made to obtain thermodynamic parameters for the equilibrium process from the experimentally observed diffusion coefficients and the crystal graphically determined radii of the tetramer and the dimer species, which in turn can be used to estimate the molar fractions of the tetramer and dimer in solution and the equilibrium constants *K* at various temperatures (see ESI). A plot of ln(K_{eq}) vs 1/T reveals a endothermic reaction process whit the following parameters: ΔH° = 70.4(±9.22) kJ mol^{-1}, ΔS° = 259(±29.5) J K^{-1} mol^{-1} and ΔG°_{298}= -6.97 (±12.7) kJ mol^{-1}.

While these values are only estimates, and no substantial emphasis should be placed on them, ~~however these~~the values may be compared with those found for other dimer—tetramer equilibrium process[79] and indicate, that in this instance, tetramer formation is significantly favoured at lower temperatures.

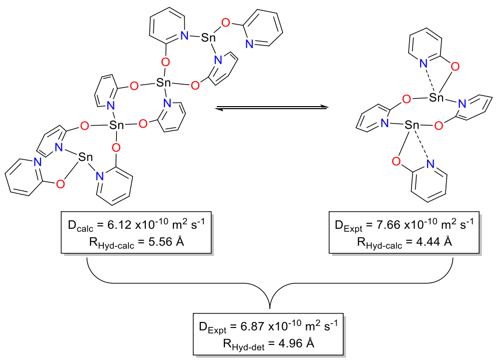

Scheme 2. Proposed Tetramer Dimer equilibria observed for **2**.

Table 1. Experimentally determined (^{1}H DOSY NMR) diffusion coefficients (D), calculated Hydrodynamic radii ($R_{Hyd-cal}$) and calculated Molecular volume (V_{cal}) of **2** at temperatures between 298-348 K.

Temp (K)	D (m^2s^{-1})	$R_{Hyd-cal}$ (Å)	V_{cal} (Å^3)
298	7.974 x^{-10} ~~E-10~~	4.93	503
308	9.416 x^{-10} ~~E-10~~	4.85	477
318	1.116 x^{-9} ~~E-09~~	4.70	436
328	1.310 x^{-9} ~~E-09~~	4.57	400
338	1.538 x^{-9} ~~E-09~~	4.41	360
348	1.750 x^{-9} ~~E-09~~	4.37	350

[1] Tables may have a footer.

Formatted: Superscript

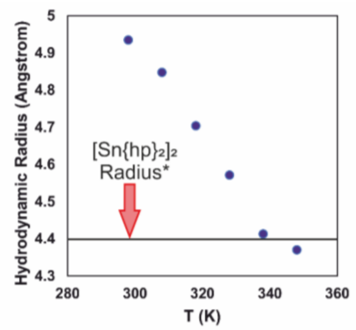

Figure 4. Graph showing the experimentally determined diffusion coefficients of **2**, 5.43mM in d^8-Tol, as a function of temperature. *: Radius (4.44 Å) as determined by single crystal X-ray diffraction.

During our investigation into the synthesis of complex **2**, crystals of a second product were serendipitously isolated from the reaction liquors, i.e., complex **3**. Unfortunately, full characterisation of **3** was not possible due to the low yield of the product and attempts to produce crystals of **3** on a larger scale to afford full unsuccessful. Only a very few pale-yellow crystals were obtained after slow (4 weeks) diffusion of air and atmospheric moisture into a solution of **2** in toluene at room temperature.[80]

Single crystal X-ray analysis of these crystals revealed the product to be an Sn(II) oxo cluster, specifically [{$Sn_6(\mu_3\text{-}O)_6(\mu\text{-}OC_5H_5N)_2(OC_5H_4N)_2$}:2{Sn($\kappa^2$ON-$OC_5H_4N)_2$}] (**3**), *vide infra*. Scheme 3 shows a possible synthetic pathway to **3**.

Field Code Changed

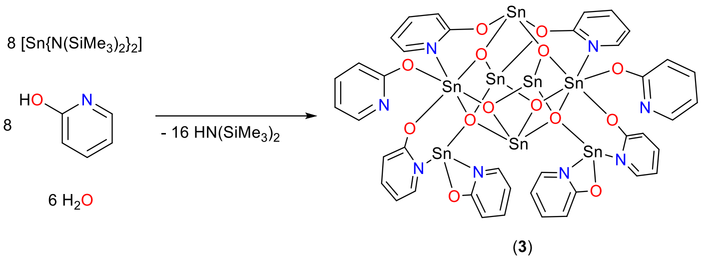

Scheme 3. Formation of the Sn(II) oxo cluster, [$Sn_6(m^3\text{-}O)_6(OR)_4$:{$Sn^{(II)}(OR)_2$}$_2$] (**3**) (R = C_5H_4N).

Reaction of [Sn{$N(SiMe_3)_2$}$_2$] with equimolar amounts of the ligands 8-hydroxyquinoline and 10-hydroxybenzo[h]quinoline respectively (Scheme 34), results in the formation of the *bis*-quinolinato complexes, **4**-**5**, in yields <50%, suggestive of an equilibrium in which the putative mono-amide intermediates are unstable with respect to disproportionation, and formation of the *bis*-complex.

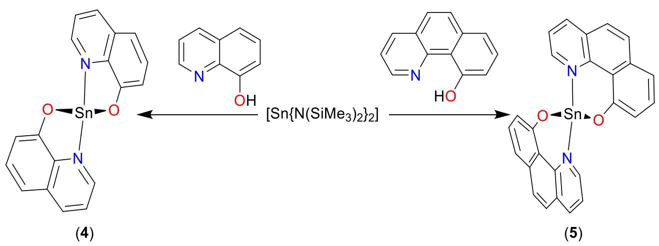

Scheme 34. The synthesis of complexes **4** and **5**.

In both cases (**4** and **5**) the ^{1}H and ^{13}C{^{1}H} NMR spectra display a series of multiplet resonances in the aromatic region. The intrinsic C_2-symmetry of complexes **4**-**5** (Scheme 34) is negated somewhat in solution by a rapid, so-called, "*flip-flop*" equilibrium process in which the N→Sn coordination bonds repeatedly open and close, a process observer for other Sn(II) systems containing *O,N* chelate ligands, resulting in a single set of resonances. The absence of a peak corresponding to the {$N(SiMe_3)_2$} group is consistent with the formation of a *bis*-substituted complexes [Sn{hq}$_2$] and [Sn{hbq}$_2$], an assertion supported by the presence in the ^{119}Sn{^{1}H} NMR spectra of single peaks at δ = -386 ppm and -542 pmm respectively. Stoichiometric reaction (2:1) of the pro-ligands hqH and hbqH, with [$Sn\{N(SiMe_3)_2\}_2$] produces the expected complexes cleanly in moderate to high yields (69-84%). Formation of the *bis*-quinolinato complexes was supported by elemental analysis.

3. Single crystal X-ray diffraction studies and Molecular Structures of Tin(II) Complexes:

X-ray diffraction studies on single crystals of complexes **1**, **2**, **4** and **5** unambiguously established their solid-state structures. The structures of the heteroleptic and homoleptic complexes, [$Sn(\mu\text{-}\kappa^2ON\text{-}OC_5H_4N)(N\{SiMe_3\}_2)]_2$ (**1**) and [$Sn_4(\mu\text{-}\kappa^2ON\text{-}OC_5H_4N)_6(\kappa^1O\text{-}OC_5H_4N)_2$] (**2**) are shown in Figures 5 and 6 respectively, with selected bond lengths and angles in Tables 2 and 3 respectively. Compound **1** (Fig. 5) exists as a centrosymmetric dimer in the solid state, comprising of two independent [{hp}$Sn\{N(SiMe_3)_2\}$] molecules in the asymmetric unit cell, with symmetry operators generating the second half of each dimer.

Both the oxygen and nitrogen donor atoms of the oxypyridinato ligands bridge the two transoidal $Sn\{N(SiMe_3)_2\}$ moieties in a head-to-tail (HT) $\mu\text{-}\eta^2$ coordination mode, resulting in an eight membered $Sn_2O_2C_2N_2$ cyclic core to the molecule.

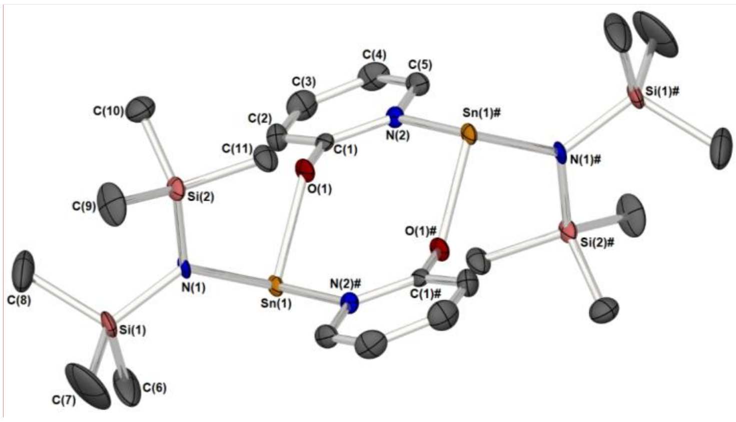

Commented [AJ3]: New higher resolution Picture

Figure 5. The molecular structure of one of the two full molecules of complex **1** present in the unit cell. Symmetry transformations used to generate equivalent atoms: #1 −X, −Y, 1−Z. Thermal ellipsoids are shown at 50% probability. Hydrogen atoms have been omitted for clarity.

Table 2. Selected bond lengths (Å) and bond angles (°) for complex **1**.

Selected Bond Lengths (Å)		Selected Bond Angles (°)	
Sn(1)-N(1)	2.1009(16)	N(1)-Sn(1)-N(2)#	90.30(7)
Sn(2)-N(3)	2.1064(16)	N(1)-Sn(1)-O(1)	93.36(6)
		O(1)-Sn(1)-N(2)#	90.72(6)
Sn(1)-O(1)	2.1491(14)		
Sn(2)-O(2)	2.1434(15)	N(3)-Sn(2)-N(4)#	90.08(7)

		N(3)-Sn(2)-O(2)	92.91(6)
Sn(1)-N(2)	2.2751(19)	O(2)-Sn(2)-N(4)#	92.46(6)
Sn(2)-N(4)	2.2590(19)		
C(1)-O(1)	1.302(3)	O(1)-C(1)-N(2)	116.7(2)
C(1)-N(2)	1.355(3)	O(2)-C(21)-N(4)	116.6(2)
C(21)-O(2)	1.302(3)		
C(21)-N(4)	1.351(3)	O(1)-C(1)-N(2)-Sn(1)#	3.2(2)
		O(2)-C(21)-N(4)-Sn(2)#	3.0(2)

Each Sn(II) centre in **1** is three-coordinate and may be regarded as being at the centre of a distorted trigonal pyramid, in which the Sn atoms are coordinated by one oxygen atom and one nitrogen atom from two different {hp} ligands in a "Head-to-Tail" fashion (see Figure 2), as well as the nitrogen of a terminal $\{N(SiMe_3)_2\}$ ligand [Sn(1)-N(1) 2.101(2)Å and Sn(2)-N(3) 2.106(2)Å]. The bond angles about each Sn(II) atom in **1** [*i.e.* N(2A)-Sn(1)-O(1) 90.71°; N(2A)-Sn(1)-N(1) 90.30°; O(1)-Sn(1)-N(1) 93.36°] suggest the absence of significant *sp*-hybridisation at tin.

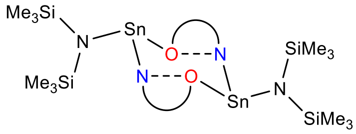

(**I**)

Scheme 5. Schematic drawing showing the coordination of the {hp} ligand in complex **1**.

The Sn–O and Sn–N bond lengths within the 8-membered ring [Sn(1)-O(2) 2.1491(14), Sn(1)-N(2) 2.2751(19) and Sn(2)-O(2) 2.1434(15), Sn(2)-N(4) 2.2590(19) Å] are shorter than the range expected for simple Sn←O and Sn ←N Lewis acid–base complexes ~~(2.1–2.4 Å)~~.[9,51,81-83] Although the pyridine rings are stacked in the crystal lattice in an antiparallel-displaced arrangement, the inter-ring distance (>4 Å) is greater than that expected for any significant electronic interaction (i.e. 3.4 Å).[84]

Furthermore, in each Sn-containing eight-membered ring, the core of the molecule adopts a chair like ring conformation similar to that observed in the pyridine-selenolate complex $[Sn_2\{\mu\text{-}\eta^2Se\text{-}2\text{-}C_5H_4N\}_2\{SeC_5H_4N\}_2]$.[85] While Sn(II) oxypyridinato complexes such as **1** have not, to the best of our knowledge, been previously reported, the core structure of **1** is reminiscent of Sn(II) carboxylate complexes $[\{Sn(NR_2)(\mu\text{-}\eta^2\text{-}O_2CAr)_2\}]$ (Ar = *m*-terphenyl).[86] As the bridging ligand oxypyridinato is isolobal to a carboxylate ligand $[O_2CR]$, this comparison is unsurprising. Similarly, **1** is also reminiscent of the *bis*(trimethylsilyl)amido Sn(II) triflate $[\{Sn(NR_2)(\mu\text{-}\eta^2\text{-}OTf)_2\}]$ complex, which also ~~contains~~ consists of a Sn-containing eight-membered heterocyclic ring.[83] However, unlike the triflate derivative, complex **1** is a discrete entity, and shows no evidence of intermolecular Sn···O interactions between adjacent eight membered rings. The puckering of the central $\{Sn_2O_2C_2N_2\}$ ring may be considered to be as a result of folding of the eight-membered ring along the two inter-ligand O···N vectors, such that it adopts a chair-like conformation (**I**) (Scheme ~~4~~5). The extent of folding (θ_{ring}) may be defined as the angle between the {SnON} planes and the $\{O_2N_2\}$ plane. In the absence of steric interactions, the "ideal" folding angle (θ_{ring}) should be ca. 130°; the fold angle in **1** is θ_{ring} = 129.14°. A similar bonding arrangement for the μ_2-O,N hydroxypyridine ligand is observed in the aluminium complex $[(^tBu)_2Al(\mu\text{-}O\text{-}2\text{-}C_5H_4N)]_2$.[70]

Commented [AJ4]: The range has been removed to avoid confusion and the readers are directed towards the accociated references.

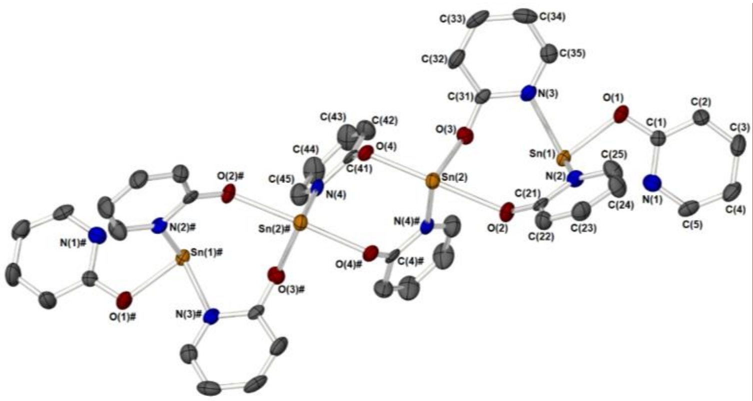

Figure 6. The solid state molecular structure of complex **2**. Symmetry transformations used to generate equivalent atoms: #1 3/2−X, Y, 1−Z. Thermal ellipsoids are shown at 50% probability. Hydrogen atoms have been omitted for clarity.

Commented [AJ5]: New higher resolution Picture

The molecular structure of **2** is shown in Figure 6 and comprises of a series of three eight-membered *spiro*-$Sn_2O_2C_2N_2$ rings that link through the Sn centres to create a one-dimensional three-link chain; selected bond lengths and angles are given in Table 3. Compound **2** is tetrameric, containing four Sn atoms and eight oxypyridinato ligands with three different coordination modes; two {hp} ligands are observed in terminal positions coordinating to the two 3-coordinate Sn(II) centres via the oxygen atom of the {hp} ligand. Two oxypyridinato ligands in the central 8-membered ring bridge two 4-coordinate Sn(II) centres in a μ−η² head-to-tail (HT) coordination mode. The four remaining oxypyridinato ligands bridge between the two 4-coordiate Sn(II) centre in the central 8-membered ring and the two three-coordinate Sn(II) centres in a μ−η² head-to-head (HH) coordination mode.

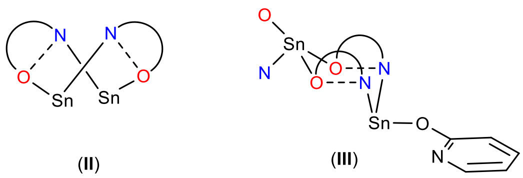

Scheme 6. Schematic drawing showing the coordination of the {hp} ligands in complex **2**

At the centre of complex **2** is a {$Sn_2O_2C_2N_2$} ring comparable in coordination geometry to that observed in complex **1**; the central ring in complex **2** can be considered to be in a boat-like conformation (**II**) (Scheme ~~5~~6) resulting from a folding along Sn···O vectors such that the two pyridine rings tend towards co-planarity, with an angle between the {$SnONC_5$} planes of 35.36° and an inter-ring distance of 3.760(2) Å. As result of this puckering the Sn···Sn distance in the inner ring is marginally reduced to 4.082 Å (cf. 4.468 Å in **1**).

Both Sn(II) centres in this central ring are four coordinate, and may be considered to be the spiro atoms linking the three 8-membered {$SnN_2C_2O_2Sn$} rings together. While the two Sn(II) centres are 4-coordinate their geometry may be regarded as either distorted trigonal bipyramidal with a stereo-active lone pair of electrons, or disphenoidal.

Table 3. Selected bond lengths (Å) and bond angles (°) for complex **2**.

Selected Bond Lengths (Å)		Selected Bond Angles (°)	
Sn(1)-O(1)	2.135(3)	N(2)-Sn(1)-N(3)	86.64(13)
Sn(1)-N(2)	2.239(4)	O(1)-Sn(1)-N(2)	87.04(14)
Sn(1)-N(3)	2.337(4)	O(1)-Sn(1)-N(3)	79.58(13)
Sn(2)-O(2)	2.370(3)	O(2)-Sn(2)-O(4)	157.89(13)
Sn(2)-O(3)	2.142(3)	O(3)-Sn(2)-N(4)#	83.40(14)
Sn(2)-O(4)	2.263(3)	O(2)-Sn(2)-O(3)	78.57(12)
Sn(2)-N(4)#	2.230(4)	O(2)-Sn(2)-N(4)#	78.58(13)
		O(3)-Sn(2)-O(4)	86.85(12)
O(1)-C(1)	1.322(5)	O(4)-Sn(2)-N(4)#	83.35(12)
C(1)-N(1)	1.333(6)	O(1)-C(1)-N(1)	116.5(4)
O(2)-C(21)	1.289(6)	O(2)-C(21)-N(2)	116.1(4)
C(21)-N(2)	1.357(6)	O(3)-C(31)-N(3)	116.6(4)
O(3)-C(31)	1.310(6)	O(4)-C(41)-N(4)	116.4(4)
C(31)-N(3)	1.347(6)	Sn(1)-O(1)-C(1)-N(1)	6.8(5)
O(4)-C(41)	1.297(6)	Sn(1)-N(2)-C(21)-O(2)	0.6(5)
C(41)-N(4)	1.348(6)	Sn(1)-N(3)-C(31)-O(3)	2.3(5)
		Sn(2)#-N(4)-C(41)-O(4)	0.4(4)

As noted above the two outer {$SnN_2C_2O_2Sn$} rings are different to the central ring with the oxypyridinato ligands bridging the two Sn(II) centres in the outer rings in head-to-head bridging modes. The puckering of the "outer" $Sn_2O_2C_2N_2$ rings may be considered to be chair like (**III**) (Scheme 6), resulting from a folding of the eight-membered ring along the two inter-ligand O···N vectors; θ_{ring} angle between {SnO_2} plane/{O_2N_2} plane = 39.91(5)°, and between {O_2N_2} plane/{SnN_2} plane = 97.92(5)°, thus resulting in a solid state arrangement such that the 3-coordinate Sn(II) centers are folded under the {O_2N_2} plane (see (**III**) in Scheme 6).

The Sn–O and Sn–N bond lengths within both the three 8-membered rings and the exo-Sn-O bonds are within expected ranges for these complexes. Similarly, bond lengths and bond angles within the oxypyridinato ligands are all similar and within parameters observed in related complexes (*vide supra*).

While for complex **1** there are no comparable mono thio- or seleno-pyidinato complexes with which the coordination chemistry of oxy-pryidinato {hp} ligand can be compared, the homoleptic *bis*-thio and *bis*-seleno- complexes, [Sn{S-C_5NH_4}$_2$] [87] and [Sn{Se-C_5NH_4}$_2$][85] are known, and display a different structural chemistry to their oxygen containing cousin, **2**. Similarly, the homoleptic lead(II) 3,5-dinitro-2-pyridonate complex possess polymeric 1D solid state structure, consisting of a {Pb_2O_2} core.[73]

As noted above, during our investigation into the synthesis of complex **2**, crystals of a second product ~~were serendipitously~~ isolated from the reaction liquors. Single crystal X-ray analysis of these crystals revealed the product to be ~~an~~ the Sn(II) oxo cluster, ~~specifically~~ [{$Sn_6(\mu_3\text{-}O)_6(\mu\text{-}OC_5H_5N)_2(OC_5H_4N)_2$}:2{$Sn(\kappa^2ON\text{-}OC_5H_4N)_2$}] (**3**), ~~in~~ which is composed of a central {Sn_6O_6} core supported by four {hp} ligands, two of which are coordinated in a N,O-μ-η² coordination mode, and two of which are terminal (Scheme 6). The cluster is further appended by the coordination of two [Sn{hp}$_2$] moieties, previously unobserved in this study, via a dative O←Sn interaction between two {μ$_3$-O} groups of the {Sn$_6$O$_6$} cluster and the Sn atoms of [Sn{hp}$_2$] units (Scheme 3).

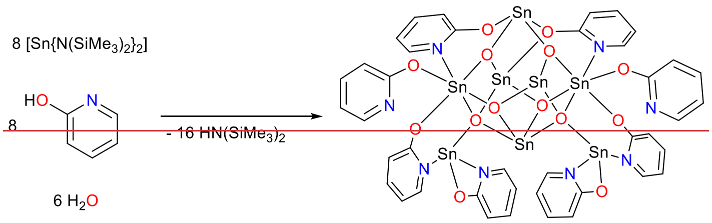

(**3**)

Scheme 6. Formation of the Sn(II) oxo cluster, [Sn$_6$(m^3-O)$_6$(OR)$_4$:{Sn$^{(II)}$(OR)$_2$}$_2$] (**3**) (R = C_5H_4N).

While the principal {Sn$_6$O$_6$} core is comparable to other Sn(II) oxo-alkoxide systems,[88] to the best of our knowledge, this is the first example of any such a cluster engaging in exo-coordinating to any metal centre via a dative M←{μ$_3$-O} interaction, rather than a Sn(II) centre.[89-92] The molecular structure of complex **3** is shown in the supplementary information, along with selected bond lengths and bond angles.

Unfortunately, full characterisation of **3** was not possible due to the low yield of the product. Attempts to produce crystals of **3** on a larger scale to afford full characterisation via a controlled hydrolysis of [Sn{N(SiMe$_3$)$_2$}] in the presence of hydroxypyridine were unsuccessful.[80] Only a very few pale yellow crystals were obtained after slow (4 weeks) diffusion of air and atmospheric moisture into a solution of **2** in toluene at room temperature.

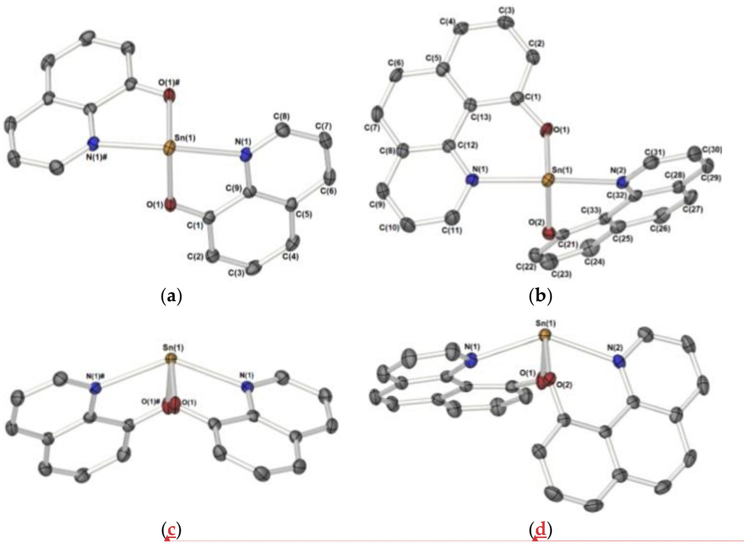

Formatted: Font: Bold

Formatted: Font: Bold

Figure 7. The molecular structure of **4** (a & c) and **5** (b & d). Thermal ellipsoids are shown at 50% probability. H-atoms are omitted for clarity. Solvent of crystallization (toluene) in ~~4~~ 5 is omitted for clarity. Symmetry transformations used to generate equivalent atoms: #1 3/2−X, Y, 1−Z.

The solid-state molecular structures of **4** and **5**, ~~were obtained~~as determined by single crystal X-ray crystallography are shown in Figure 7, with selected bond distances (Å) and bond angles (°) in Table 4. Complex **3** crystallises in orthorhombic space group *Pbcn* with half of the molecular complex in the asymmetric unit. Contrastingly, complex **5** crystallises in the triclinic space group *P-1* with one full molecule in the unit cell alongside one whole molecule of disordered toluene.

Formatted: Font: Not Bold

The solid-state structures of **4** and **5** are consistent with the spectroscopic data suggesting the monomeric structures of the complexes in the solid state are retained in solution. Both complexes have what may be described as "two-bladed propeller" like geometry, with a C_2 axis lying on the bisectors of the N–Sn–N axis. Whilst **3** and **4** are both chiral, by virtue of their molecular C_2 symmetry, the enantiomers co-crystallise in non-centrosymmetric space groups.

Table 4. Selected bond lengths (Å) and bond angles (°) for complexes **4** and **5**.

4		**5**	
Selected Bond Lengths (Å)			
Sn(1)-O(1)	2.0985(17)	Sn(1)-O(1)	2.0824(15)
		Sn(1)-O(2)	2.0779(17)
Sn(1)-N(1)	2.4014(19)	Sn(1)-N(1)	2.4140(19)
		Sn(1)-N(2)	2.4289(19)
O(1)-C(1)	1.326(3)	O(1)-C(1)	1.328(3)
		O(2)-C(21)	1.326(3)
Selected bond angles (°) [1]			

N(1)-Sn(1)-N(1)#	138.54(9)	N(1)-Sn(1)-N(2)	141.52(7)
O(1)-Sn(1)-O(1)#	98.23(10)	O(1)-Sn(1)-O(2)	97.33(7)

[1] # denotes symmetry generated atom (#: 3/2−X, Y, 1−Z).

Despite coordination numbers of four, in both **4** and **5**, analysis of the N-Sn-N and O-Sn-O bond angles about the Sn(II) centres suggests ~~a~~ the Sn atoms in adopt a pseudo trigonal bipyramidal, or disphenoidal geometry, each with a stereoactive lone pair of electrons [**4**: τ = 0.67, **5**: τ = 0.74] in which with the nitrogen atoms occupying the axial coordination sites and oxygen atoms the equatorial positions. While the N–Sn–N bond angles increase from ~138.5° to 141.5° as the chelate ring is changed from 1,4-κ²N,O, to 1,5-κ²N,O coordination respectively. The associated O–Sn–O angles [**4**: 98.224(17)°, **5**: 97.331(14)°] are both close 90°, suggesting that the Sn–O bonds are largely based around the Sn(II) *p*-orbitals. The 1,4-κ²N,O and 1,5-κ²N,O coordination of the ligands are associated with acute bite angles (N–Sn–O) of 73.23(2)° for **4** and 74.76(3)/77.07(3)° for **5** and induce a distortion of the axial vector (N–Sn–N) from linearity to angles of 138.56(2)° and 141.52(5)° for **4** and **5**, respectively

In complex **4** and **5**, the Sn–O distances (**4**: 2.0985(17)Å; **5**: 2.0824(15) and 2.0779(17)Å) are slightly shorter than comparable Sn–O interactions in complexes **1** and **2**. For **4** Sn-O and Sn-N bond lengths are comparable to related systems (*vide supra*). Contrastingly, the Sn–N interactions in **4** and **5** (2.4014(19)Å and 2.4140(19)/2.4289(19)Å) are slightly longer than those observed in **1** and **2**. However both Sn-O and Sn-N bond lengths are in good agreement with the interatomic distances reported for comparable Sn(II) O-N chelate complexes (*vide supra)*.

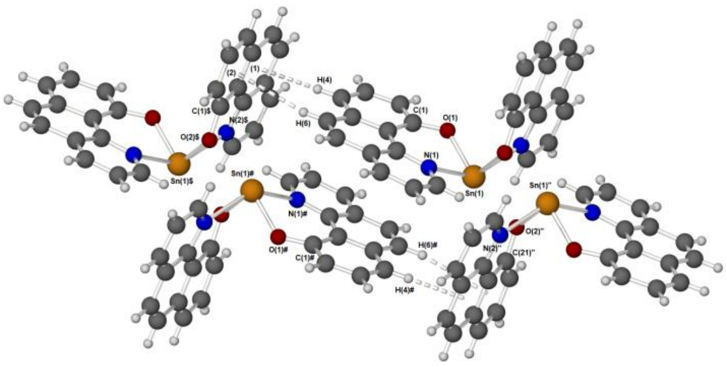

Figure 8. A representation of the H-Bonding and π-π stacking observed in the solid-state structure of **5**. Bond lengths: H(4)-(1)$_{cent}$ = 2.658(12)Å and H(6)-(2)$_{cent}$ = 3.227(12)Å. Interplane distance: {C(1)-N(1)}/{C(1)#-CN(1)# = 3.687(12)Å. Symmetry transformations used to generate equivalent atoms: #1: X-1, 1+Y, -Z; $#: X-1, 1+Y, Z;"# X-1, 1+Y, Z.

As noted previously, complex **4** possesses molecular C_2 symmetry. In contrast, one of the {hbq} ligands is folded along the inter-ligand O(1)···N(2) vectors such that the three-rings of the {hbq} ligand are moved away from the second {hbq} ligand. A closer inspection of the intermolecular distances associated with complex **5** reveals both favourable π-π stacking interactions, between the {C(1)-N(1)} and {C(1)#-N(1)#} poly-aromatic rings, [3.687(12)Å between the parallel planes defined by the atoms {C(1)-N(1)} and {C(1)#-N(1)#} respectively], and C-H···π interactions between adjacent molecules as shown in

Figure 8, [H(4)-(1)$_{cent}$ = 2.658(12)Å and H(6)-(2)$_{cent}$ = 3.227(12)Å], which are presumably the origin of the observed distortion from molecular C_2 symmetry in the solid state. Interestingly complex **5** appears to one of a small number of structurally characterized examples of the {hbq} ligand coordinated to a metal centre, other than [Be{hbq}$_2$][93] [Me_2Ga{hbq}] and [Me_2In{hbq}]$_2$,[94] reported in the literature.

4. Conclusions

In recent years 1,3-O,N, 1,4-O,N, and to a lesser extent 1,5-O,N chelate ligands based around the "basic" oxo-pyridinato system have been shown to play an important role as sterically and electronically tuneable ligands to a range of metal centres. The ambidentate nature of these tuneable ligands has allowed the stabilisation of metals spanning most the periodic table. However, there is a paucity of main group metal examples bearing such ligands. Here, we describe an explorative investigation into the chemistry of these systems and highlight the array of reactive and novel bonding modes such versatile ligands display in a family of Sn(II) complexes bearing the pyridinato ligands oxopyridinato {hp} (**1** and **2**), quinolinato, {hq} (**3**) and oxybenzo[h]quinolinato {hbq} (**4**). The Sn(II) complexes bearing these ligands were synthesized and characterised in solution and in the solid state. In the case of the 1,3-κ^{2}NO oxpyridinato systems, the ligand displays a diverse coordination geometry, mirroring some observations made in transition metal chemistry. In contrast, the coordination chemistry of the quinolinato, {hq} and oxybenzo[h]quinolinato {hbq} ligands display a much more limited variety in their bonding modes with **3** and **4** displaying distorted trigonal bipyramidal geometries. To the best of our knowledge complexes **1**, **2** are the first reported examples Sn(II) centres supported by oxo-pyridinato ligands. In addition, complex **5** is a rare example of a coordination complex of the oxybenzo[h]quinolinato (**5**) ligands, and as such, one of only a small number from across the whole of the periodic table.

5. Experimental Section

Experimental Details: ^{1}H, ^{13}C and ^{119}Sn NMR spectra were recorded on Bruker Avance 300 or 500 MHz FT-NMR spectrometers, as appropriate, in saturated solutions at room temperature. Chemical shifts are expressed in ppm with respect to Me_4Si (^{1}H and ^{13}C) and SnMe4 (^{119}Sn) in C_6D_6. Elemental Analysis was performed externally by London Metropolitan University Elemental Analysis Service.

All reactions were carried out under an inert atmosphere using standard Schlenk techniques. Solvents were dried and degassed under an argon atmosphere over activated alumina columns using an Innovative Technology solvent purification system (SPS). The Sn(II) amide, [Sn{N($SiMe_3$)$_2$}$_2$], was prepared by literature methods.[95]

Synthesis of [Sn(μ–κ^{2}ON-OC_5H_4N)(N{$SiMe_3$}$_2$)]$_2$ (1): To a cooled solution of [Sn{N($SiMe_3$)$_2$}$_2$] (1 mmol, 0.44 g) in Ttoluene (10 ml) a suspension of 2-hydroxypyridine (1 mmol, 0.10 g) in toluene (10 ml) was added and stirred for 2 hrs. The resulting solution gradually became yellow in colour. The reaction mixture was heated to near reflux and filtered through a Celite® pad (hot) to afford a clear pale-yellow filtrate. Removal of excess solvent under vacuum followed by storage at -28 °C yielded 0.20 g pale yellow microcrystals crystals (Yield = 54 %). Elemental Analysis ($C_{11}H_{22}N_2OSi_2Sn$)$_2$ (expected): C 35.59% (35.40%), H 6.02% (5.94%), N 7.51% (7.51%). 1H NMR (C_6D_6, 500 MHz): δ 0.37 (s, 18H, -N{$SiMe_3$}$_2$), 6.19-6.23 (m, 1H, 5-CH), 6.47-6.50 (m, 1H, 3-CH), 6.94-6.99 (m, 1H, 4-CH), 7.97-8.01 (m, 1H, 6-CH). ^{13}C NMR (C_6D_6, 125.7 MHz): δ 6.0 (-N{$SiMe_3$}$_2$), 114.0 (5-C), 116.6 (3-C), 142.2 (4-C), 142.6 (6-C), 170.0 (2-C). ^{119}Sn NMR (C_6D_6, 186.5 MHz): δ –85.

Synthesis of $[Sn_4(\mu\text{-}\kappa^2ON\text{-}OC_5H_4N)_6(\kappa^1O\text{-}OC_5H_4N)_2]$ (2): To a cooled solution of $[Sn\{N(SiMe_3)_2\}_2]$ (2 mmol, 0.88 g) in toluene (10 ml) a suspension of 2-Hydroxypyridine (4 mmol, 1.23 g) in toluene (10 ml) was added. A colourless precipitate was observed formed over time. The suspension was allowed to stir for 2 hours before the precipitate was heated into solution. Filtration through a Celite® pad afforded a colourless filtrate. Slow cooling (-28 °C) afforded 0.58 g of small starburst colourless crystals. (yield = 94%). Elemental Analysis $(C_{10}H_8N_2O_2Sn)_4$ (expected): C 38. 7% (39.14%), H 2.85% (2.63%), N 9.11% (9.13%). ^{1}H NMR (C_6D_6, 500 MHz): δ 5.98-6.05 (m, 1H, 5-CH), 6.54-6.61 (m, 1H, 3-CH), 6.88-6.95 (m, 1H, 4-CH), 7.58-7.67 (m, 1H, 6-CH). ^{13}C NMR (C_6D_6, 125.7 MHz): δ 112.71 (5-C), 115.70 (3-C), 140.44 (4-C), 143.73 (6-C), 19.30 (2-C). ^{119}Sn NMR (C_6D_6, 186.5 MHz): δ –526.

Synthesis of $[Sn(\mu\text{-}\kappa^2ON\text{-}OC_9H_6N)_2]$ (4): A suspension of 8-Hydroxyquinoline (4 mmol, 0.5806 g) in toluene (10 ml) was added, via cannula, to a cooled solution of cooled solution of $[Sn\{N(SiMe_3)_2\}_2]$ (2 mmol, 0.88 g) in toluene. A bright yellow precipitate was generated instantly. The suspension was allowed to stir for 2 hours before the precipitate was heated into solution and filtered through a Celite® pad affording a yellow filtrate. Slow cooling (-28 °C) afforded 0.62g of large yellow crystals. (yield = 76%). Elemental Analysis $C_{18}H_{12}N_2O_2Sn$ (expected): C 53.27% (53.12%), H 3.02% (2.97%), N 6.85% (6.88%). ^{1}H NMR (C_6D_6, 500 MHz): δ 8.32 (d, $J^3_{H\text{-}H}$ = 5Hz, 1H 2-CH) 7.45 (d, $J^3_{H\text{-}H}$ = 10Hz, 1H, 7-CH) 7.19 (dd, $J^3_{H\text{-}H}$ = 10Hz, $J^3_{H\text{-}H}$ = 10Hz, 1H, 3-CH), 7.10 (dd, $J^3_{H\text{-}H}$ = 10Hz, $J^3_{H\text{-}H}$ = 5Hz, 1H, 6-CH), 6.69 (d, $J^3_{H\text{-}H}$ = 10Hz, $J^3_{H\text{-}H}$ = 10Hz, 1H, 4-CH), 6.61 (dd, (dd, $J^3_{H\text{-}H}$ = 5Hz, $J^3_{H\text{-}H}$ = 5Hz, 1H, 5-CH). ^{13}C NMR (C_6D_6, 125.7 MHz): δ 112.6 (4-C), 115.2 (6-C), 121.0 (5-C), 130.6 (3-C), 130.8 (8-C), 138.4 (7-C), 140.2 (9-C), 143.3 (2-C), 162.9 (1-C).^{119}Sn NMR (C_6D_6, 186.5 MHz): δ –386.

Synthesis of $[Sn(\mu\text{-}\kappa^2ON\text{-}OC_{13}H_8N)_2]$ (5): A suspension of 10-Hydroxybenzo[h]quinoline (4 mmol, 0.7810 g) in toluene (10 ml) was added, via cannula, to a cooled solution of cooled solution of $[Sn\{N(SiMe_3)_2\}_2]$ (2 mmol, 0.88 g) in toluene. A bright yellow precipitate was generated instantly. The suspension was stirred for 2 hours before the precipitate was heated into solution and filtered through a Celite® pad affording a yellow filtrate. Slow cooling (-28 °C) afforded 0.62g of large yellow crystals. (yield = 85%). Elemental Analysis $C_{26}H_{16}N_2O_2Sn{:}C_7H_8$ (expected): C 65.97% (66.04%), H 4.11% (4.03%), N 4.65% (4.66%). ^{1}H NMR (C_6D_6, 500 MHz): δ 6.67 (dd, $J^3_{H\text{-}H}$ = 10Hz, 5Hz, 1H, CH), 6.83 (dd, $J^3_{H\text{-}H}$ = 5Hz, 2Hz, 2H, CH), 6.91 (dd, $J^3_{H\text{-}H}$ = 10Hz, 10Hz, 1H, CH), 6.99-7.03 (m 2H CH), 7.22 (d, $J^3_{H\text{-}H}$ = 2Hz, 1H, CH), 8.08 (dd, $J^3_{H\text{-}H}$ = 5Hz, 2Hz, 1H, CH), 8.79 (dd, $J^3_{H\text{-}H}$ = 5Hz, 2Hz, 1H, CH). ^{13}C NMR (C_6D_6, 125.7 MHz): δ 116.9, 118.3, 120.0, 120.3, 120.7, 123.0, 125.6, 126.3, 126.7, 130.6, 145.0 145.6, 169.3. ^{119}Sn NMR (C_6D_6, 186.5 MHz): δ -542.

Single Crystal X-ray Diffraction Studies:

Experimental details relating to the single-crystal X-ray crystallographic data for compounds **1–4** is summarized in Table S1 (ESI). Single crystal X-ray crystallography data were collected at 150 K on RIGAKU SuperNova Dual wavelength diffractometer equipped with an Oxford Cryostream, featuring a micro source with MoK*α* radiation (λ = 0.71073 Å) and Cu K*α* radiation (λ = 1.5418 Å). Crystals were isolated from an argon filled Schlenk flask and immersed under oil before being mounted onto the diffractometer. Structures were solved by direct methods throughout and refined on F2 data using the OLEX2 suite of programs.[30] All hydrogen atoms were included in idealized positions and refined using the riding model. Refinements were straightforward with no additional points that merit note. CCDC 2015978-2015982 contain the supplementary crystallographic data for this paper. These data can be obtained free of charge at www.ccdc.cam.ac.uk/conts/retrieving.html [or from the Cambridge Crystallographic Data Centre, 12, Union Road, Cambridge CB2 1EZ, UK; fax: + 44-1223/336-033; E-mail: deposit@ccdc.cam.ac.uk].

Supplementary Materials: The following supporting information can be downloaded at: www.mdpi.com/xxx/s1, Figure S1: title; Table S1: title; Video S1: title.

Author Contributions: Conceptualization, A.L.J.; methodology, H.S.I.S; Crystallographic analysis, A.L.J and G.K.K.; NMR Investigation, A.J.S.; writing—original draft preparation, A.L.J.; writing—review and editing, A.L.J and A.J.S.; supervision, A.L.J.; project administration, A.L.J.; funding acquisition, A.L.J. All authors have read and agreed to the published version of the manuscript

Funding: This research was funded by EPSRC, grant number EP/L0163541 and EP/G03768X/1.

Data Availability Statement: In this section, please provide details regarding where data supporting reported results can be found, including links to publicly archived datasets analyzed or generated during the study. Please refer to suggested Data Availability Statements in section "MDPI Research Data Policies" at https://www.mdpi.com/ethics. If the study did not report any data, you might add "Not applicable" here.

Acknowledgments: We thank EPSRC Doctoral Training Centre in Sustainable Chemical Technologies (CSCT) for a PhD studentship (H.S.I.S).

Conflicts of Interest: The authors declare no conflict of interest.

References

1. Lappert, M.; Protchenko, A.; Power, P.; Seeber, A. Subvalent Amides of Silicon and the Group 14 Metals. In *Metal Amide Chemistry*; John Wiley & Sons Ltd: 2008; pp. 263-326.
2. Mizuhata, Y.; Sasamori, T.; Tokitoh, N. Stable Heavier Carbene Analogues. *Chemical Reviews* **2009**, *109*, 3479-3511, doi:10.1021/cr900093s.
3. Lee, V.Y.; Sekiguchi, A. *Organometallic compounds of low-coordinate Si, Ge, Sn and Pb : from phantom species to stable compounds*; Wiley: Oxford, 2010.
4. Dias, H.V.R.; Wang, Z. Germanium-Containing Heterobicyclic 10-π-Electron Ring Systems. Synthesis and Characterization of Neutral and Cationic Germanium(II) Derivatives of Aminotroponiminates. *Journal of the American Chemical Society* **1997**, *119*, 4650-4655, doi:10.1021/ja970196b.
5. Akkari, A.; Byrne, J.J.; Saur, I.; Rima, G.; Gornitzka, H.; Barrau, J. Three coordinate divalent Group 14 element compounds with a β-diketiminate as supporting ligand L2MX [L2=PhNC(Me)CHC(Me)NPh, X=Cl, I; M=Ge, Sn]. *Journal of Organometallic Chemistry* **2001**, *622*, 190-198, doi:10.1016/s0022-328x(00)00893-7.
6. Sen, S.S.; Kritzler-Kosch, M.P.; Nagendran, S.; Roesky, H.W.; Beck, T.; Pal, A.; Herbst-Irmer, R. Synthesis of Monomeric Divalent Tin(II) Compounds with Terminal Chloride, Amide, and Triflate Substituents. *European Journal of Inorganic Chemistry* **2010**, *2010*, 5304-5311, doi:10.1002/ejic.201000803.
7. Zaitsev, K.V.; Cherepakhin, V.S.; Churakov, A.V.; Peregudov, A.S.; Tarasevich, B.N.; Egorov, M.P.; Zaitseva, G.S.; Karlov, S.S. Extending the family of stable heavier carbenes: New tetrylenes based on N,N,O-ligands. *Inorganica Chimica Acta* **2016**, *443*, 91-100, doi:10.1016/j.ica.2015.12.025.
8. Ahmet, I.Y.; Hill, M.S.; Raithby, P.R.; Johnson, A.L. Tin guanidinato complexes: oxidative control of Sn, SnS, SnSe and SnTe thin film deposition. *Dalton Transactions* **2018**, *47*, 5031-5048, doi:10.1039/c8dt00773j.
9. Parish, J.D.; Snook, M.W.; Johnson, A.L.; Kociok-Köhn, G. Synthesis, characterisation and thermal properties of Sn(ii) pyrrolide complexes. *Dalton Transactions* **2018**, *47*, 7721-7729, doi:10.1039/c8dt00490k.
10. Holt, M.S.; Wilson, W.L.; Nelson, J.H. Transition metal-tin chemistry. *Chemical Reviews* **1989**, *89*, 11-49, doi:10.1021/cr00091a002.
11. Bartolin, J.M.; Kavara, A.; Kampf, J.; Banaszak Holl, M.M. Tin-Mediated CH Activation and Cross-Coupling in a Single Flask. *Organometallics* **2006**, *25*, 4738-4740, doi:10.1021/om060388s.

12. Summerscales, O.T.; Caputo, C.A.; Knapp, C.E.; Fettinger, J.C.; Power, P.P. The Role of Group 14 Element Hydrides in the Activation of C–H Bonds in Cyclic Olefins. *Journal of the American Chemical Society* **2012**, *134*, 14595-14603, doi:10.1021/ja305853d.
13. Lai, T.Y.; Fettinger, J.C.; Power, P.P. Facile C–H Bond Metathesis Mediated by a Stannylene. *Journal of the American Chemical Society* **2018**, *140*, 5674-5677, doi:10.1021/jacs.8b01878.
14. Padělková, Z.; Nechaev, M.S.; Lyčka, A.; Holubová, J.; Zevaco, T.A.; Růžička, A. Reactivity of C,N-Chelated Stannylene with Azobenzene. *European Journal of Inorganic Chemistry* **2009**, *2009*, 2058-2061, doi:10.1002/ejic.200900181.
15. Mandal, S.K.; Roesky, H.W. Group 14 Hydrides with Low Valent Elements for Activation of Small Molecules. *Accounts of Chemical Research* **2011**, *45*, 298-307, doi:10.1021/ar2001759.
16. Stewart, C.A.; Dickie, D.A.; Moasser, B.; Kemp, R.A. Reactions of CO2 and related heteroallenes with CF3-substituted aromatic silylamines of tin. *Polyhedron* **2012**, *32*, 14-23, doi:10.1016/j.poly.2011.06.010.
17. Padělková, Z.; Švec, P.; Pejchal, V.; Růžička, A. Activation of E–Cl bonds (E = C, Si, Ge and Sn) by a C,N-chelated stannylene. *Dalton Transactions* **2013**, *42*, doi:10.1039/c3dt50278c.
18. Wildsmith, T.; Hill, M.S.; Johnson, A.L.; Kingsley, A.J.; Molloy, K.C. Exclusive formation of SnO by low temperature single-source AACVD. *Chemical Communications* **2013**, *49*, doi:10.1039/c3cc45676e.
19. Chu, T.; Nikonov, G.I. Oxidative Addition and Reductive Elimination at Main-Group Element Centers. *Chemical Reviews* **2018**, *118*, 3608-3680, doi:10.1021/acs.chemrev.7b00572.
20. Hadlington, T.J.; Driess, M.; Jones, C. Low-valent group 14 element hydride chemistry: towards catalysis. *Chemical Society Reviews* **2018**, *47*, 4176-4197, doi:10.1039/c7cs00649g.
21. Dove, A.P.; Gibson, V.C.; Marshall, E.L.; White, A.J.P.; Williams, D.J. A well defined tin(ii) initiator for the living polymerisation of lactide. *Chemical Communications* **2001**, 283-284, doi:10.1039/b008770j.
22. Kim, S.B.; Sinsermsuksakul, P.; Hock, A.S.; Pike, R.D.; Gordon, R.G. Synthesis of N-Heterocyclic Stannylene (Sn(II)) and Germylene (Ge(II)) and a Sn(II) Amidinate and Their Application as Precursors for Atomic Layer Deposition. *Chemistry of Materials* **2014**, *26*, 3065-3073, doi:10.1021/cm403901y.
23. Catherall, A.L.; Harris, S.; Hill, M.S.; Johnson, A.L.; Mahon, M.F. Deposition of SnS Thin Films from Sn(II) Thioamidate Precursors. *Crystal Growth & Design* **2017**, *17*, 5544-5551, doi:10.1021/acs.cgd.7b01100.
24. Kim, H.-S.; Jung, E.A.; Han, S.H.; Han, J.H.; Park, B.K.; Kim, C.G.; Chung, T.-M. Germanium Compounds Containing Ge═E Double Bonds (E = S, Se, Te) as Single-Source Precursors for Germanium Chalcogenide Materials. *Inorganic Chemistry* **2017**, *56*, 4084-4092, doi:10.1021/acs.inorgchem.6b02697.
25. Ahmet, I.Y.; Thompson, J.R.; Johnson, A.L. Oxidative Addition to Sn(II) Guanidinate Complexes: Precursors to Tin(II) Chalcogenide Nanocrystals. *European Journal of Inorganic Chemistry* **2018**, *2018*, 1670-1678, doi:10.1002/ejic.201800071.
26. Park, J.-H.; Kang, S.G.; Lee, Y.K.; Chung, T.-M.; Park, B.K.; Kim, C.G. Tin(II) Aminothiolate and Tin(IV) Aminothiolate Selenide Compounds as Single-Source Precursors for Tin Chalcogenide Materials. *Inorganic Chemistry* **2020**, *59*, 3513-3517, doi:10.1021/acs.inorgchem.9b03369.
27. Foley, S.R.; Yap, G.P.A.; Richeson, D.S. Oxidative addition to M(II) (M = Ge, Sn) amidinate complexes: routes to group 14 chalcogenolates with hypervalent coordination environments. *Journal of the Chemical Society, Dalton Transactions* **2000**, 1663-1668, doi:10.1039/a909228e.
28. Nimitsiriwat, N.; Gibson, V.C.; Marshall, E.L.; White, A.J.P.; Dale, S.H.; Elsegood, M.R.J. Tert-butylamidinate tin(ii) complexes: high activity, single-site initiators for the controlled production of polylactide. *Dalton Transactions* **2007**, doi:10.1039/b706663e.
29. Chlupatý, T.; Růžičková, Z.; Horáček, M.; Alonso, M.; De Proft, F.; Kampová, H.; Brus, J.; Růžička, A. Oxidative Additions of Homoleptic Tin(II) Amidinate. *Organometallics* **2015**, *34*, 606-615, doi:10.1021/om501074m.

30. Chlupatý, T.; Padělková, Z.; DeProft, F.; Willem, R.; Růžička, A. Addition of Lappert's Stannylenes to Carbodiimides, Providing a New Class of Tin(II) Guanidinates. *Organometallics* **2012**, *31*, 2203-2211, doi:10.1021/om201118m.
31. Barman, M.K.; Baishya, A.; Peddarao, T.; Nembenna, S. Guanidinate stabilized germanium(II) and tin(II) amide complexes and their catalytic activity for aryl isocyanate cyclization. *Journal of Organometallic Chemistry* **2014**, *772-773*, 265-270, doi:10.1016/j.jorganchem.2014.09.030.
32. Chlupatý, T.; Růžičková, Z.; Horáček, M.; Merna, J.; Alonso, M.; De Proft, F.; Růžička, A. Reactivity of Tin(II) Guanidinate with 1,2- and 1,3-Diones: Oxidative Cycloaddition or Ligand Substitution ? *Organometallics* **2014**, *34*, 2202-2211, doi:10.1021/om500873a.
33. Ungpittagul, T.; Wongmahasirikun, P.; Phomphrai, K. Synthesis and characterization of guanidinate tin(ii) complexes for ring-opening polymerization of cyclic esters. *Dalton Transactions* **2020**, *49*, 8460-8471, doi:10.1039/d0dt01115k.
34. Dove, A.P.; Gibson, V.C.; Marshall, E.L.; Rzepa, H.S.; White, A.J.P.; Williams, D.J. Synthetic, Structural, Mechanistic, and Computational Studies on Single-Site β-Diketiminate Tin(II) Initiators for the Polymerization ofrac-Lactide. *Journal of the American Chemical Society* **2006**, *128*, 9834-9843, doi:10.1021/ja061400a.
35. Jana, A.; Roesky, H.W.; Schulzke, C. Hydrostannylation of Ketones and Alkynes with LSnH [L = HC(CMeNAr)2, Ar = 2,6-iPr2C6H3]. *Inorganic Chemistry* **2009**, *48*, 9543-9548, doi:10.1021/ic9012069.
36. Jana, A.; Objartel, I.; Roesky, H.W.; Stalke, D. Reaction of β-diketiminate tin(ii) dimethylamide LSnNMe2 [L = HC(CMeNAr)2; Ar = 2,6-iPr2C6H3] with ketones and alkynes. *Dalton Transactions* **2010**, *39*, doi:10.1039/c002849e.
37. Harris, L.A.M.; Coles, M.P.; Fulton, J.R. Synthesis and reactivity of tin amide complexes. *Inorganica Chimica Acta* **2011**, *369*, 97-102, doi:10.1016/j.ica.2010.12.009.
38. Taylor, M.J.; Saunders, A.J.; Coles, M.P.; Fulton, J.R. Low-Coordinate Tin and Lead Cations. *Organometallics* **2011**, *30*, 1334-1339, doi:10.1021/om100712a.
39. Harris, L.A.M.; Tam, E.C.Y.; Coles, M.P.; Fulton, J.R. Lead and tin β-diketiminato amido/anilido complexes: competitive nucleophilic reactivity at the β-diketiminato γ-carbon. *Dalton Transactions* **2014**, *43*, doi:10.1039/c4dt01714e.
40. Zemlyansky, N.N.; Borisova, I.V.; Kuznetsova, M.G.; Khrustalev, V.N.; Ustynyuk, Y.A.; Nechaev, M.S.; Lunin, V.V.; Barrau, J.; Rima, G. New stable germylenes, stannylenes, and related compounds. 1. Stable germanium(II) and tin(II) compounds M(OCH2CH2NMe2)(2) (M = Ge, Sn) with intramolecular coordination metal-nitrogen bonds. Synthesis and structure. *Organometallics* **2003**, *22*, 1675-1681, doi:10.1021/om020719a.
41. Khrustalev, V.N.; Portnyagin, I.A.; Zemlyansky, N.N.; Borisova, I.V.; Nechaev, M.S.; Ustynyuk, Y.A.; Antipin, M.Y.; Lunin, V. New stable germylenes, stannylenes, and related compounds 6. Heteroleptic germanium(II) and tin(II) compounds [(SiMe3)(2)N-E-14-OCH(2)CH(2)NMe2](n) (E-14 = Ge, n = 1; Sn, n = 2): synthesis and structure. *Journal of Organometallic Chemistry* **2005**, *690*, 1172-1177, doi:10.1016/j.jorganchem.2004.11.024.
42. Khrustalev, V.N.; Portnyagin, I.A.; Zemlyansky, N.N.; Borisova, I.V.; Ustynyuk, Y.A.; Antipin, M.Y. New stable germylenes, stannylenes, and related compounds. 5. Germanium(II) and tin(II) azides [N-3-E-14-OCH2CH2NMe2](2) (E-14 = Ge, Sn): synthesis and structure. *Journal of Organometallic Chemistry* **2005**, *690*, 1056-1062, doi:10.1016/j.jorganchem.2004.09.091.
43. Hollingsworth, N.; Horley, G.A.; Mazhar, M.; Mahon, M.F.; Molloy, K.C.; Haycock, P.W.; Myers, C.P.; Critchlow, G.W. Tin(II) aminoalkoxides and heterobimetallic derivatives: the structures of Sn6(O)4(dmae)4, Sn6(O)4(OEt)4 and [Sn(dmae)2Cd(acac)2]2. *Appl Organomet Chem* **2006**, *20*, 687-695, doi:10.1002/aoc.1118.
44. Khrustalev, V.N.; Glukhov, I.V.; Borisova, I.V.; Zemlyansky, N.N. New stable germylenes, stannylenes, and related compounds. 8. Amidogermanium(II) and -tin(II) chlorides R2N-E-14-Cl (E-14 = Ge, R = Et; E-14 = Sn, R = Me) revealing new structural motifs. *Appl Organomet Chem* **2007**, *21*, 551-556, doi:10.1002/aoc.1252.

45. Khrustalev, V.N.; Zemlyansky, N.N.; Borisova, I.V.; Kuznetsova, M.G.; Krut'ko, E.B.; Antipin, M.Y. New stable germylenes, stannylenes, and related compounds 7.* Synthesis and structures of compounds. *Russ Chem B+* **2007**, *56*, 267-270, doi:DOI 10.1007/s11172-007-0043-y.
46. Aysin, R.R.; Leites, L.A.; Bukalov, S.S.; Khrustalev, V.N.; Borisova, I.V.; Zemlyanskii, N.N.; Smirnov, A.Y.; Nechaev, M.S. Vibrational spectra and structural features of carbene analogs El(II)(OCH2CH2NMe2)(2) and ClEl(II)OCH(2)CH(2)NMe(2) (El(II) = Ge, Sn, Pb). *Russ Chem B+* **2011**, *60*, 69-80, doi:DOI 10.1007/s11172-011-0010-5.
47. Han, J.H.; Chung, Y.J.; Park, B.K.; Kim, S.K.; Kim, H.-S.; Kim, C.G.; Chung, T.-M. Growth of p-Type Tin(II) Monoxide Thin Films by Atomic Layer Deposition from Bis(1-dimethylamino-2-methyl-2propoxy)tin and H2O. *Chemistry of Materials* **2014**, *26*, 6088-6091, doi:10.1021/cm503112v.
48. Han, S.H.; Jung, E.A.; Lee, J.H.; Kim, D.H.; Lee, G.Y.; Park, B.K.; Kim, C.G.; Son, S.U.; Chung, T.M. Synthesis and Structure of Novel Tin Complexes Containing Aminoalkoxide Ligands. *ChemistrySelect* **2018**, *3*, 7836-7839, doi:10.1002/slct.201801375.
49. Wang, L.; Kefalidis, C.E.; Roisnel, T.; Sinbandhit, S.; Maron, L.; Carpentier, J.-F.; Sarazin, Y. Structure vs 119Sn NMR Chemical Shift in Three-Coordinated Tin(II) Complexes: Experimental Data and Predictive DFT Computations. *Organometallics* **2014**, *34*, 2139-2150, doi:10.1021/om5007566.
50. Alvarez-Rodriguez, L.; Cabeza, J.A.; Garcia-Alvarez, P.; Polo, D. Organic Amides as Suitable Precursors to Stabilize Stannylenes. *Organometallics* **2013**, *32*, 3557-3561, doi:10.1021/om400476c.
51. Nimitsiriwat, N.; Gibson, V.C.; Marshall, E.L.; Elsegood, M.R.J. The Reversible Amination of Tin(II)-Ligated Imines: Latent Initiators for the Polymerization ofrac-Lactide. *Inorganic Chemistry* **2008**, *47*, 5417-5424, doi:10.1021/ic701671s.
52. Nimitsiriwat, N.; Gibson, V.C.; Marshall, E.L.; Elsegood, M.R.J. Bidentate salicylaldiminato tin(ii) complexes and their use as lactide polymerisation initiators. *Dalton Transactions* **2009**, doi:10.1039/b812877d.
53. Piromjitpong, P.; Ratanapanee, P.; Thumrongpatanaraks, W.; Kongsaeree, P.; Phomphrai, K. Synthesis of cyclic polylactide catalysed by bis(salicylaldiminato)tin(ii) complexes. *Dalton Transactions* **2012**, *41*, doi:10.1039/c2dt31678a.
54. Kao, H.-M.; Ho, S.-M.; Chen, I.C.; Kuo, P.-C.; Lin, C.-Y.; Tu, C.-Y.; Hu, C.-H.; Huang, J.-H.; Lee, G.-H. Synthesis and structures of three, four, and six-coordinate monomeric tin(II) and tin(IV) compounds containing η2-ketiminate ligands. *Inorganica Chimica Acta* **2008**, *361*, 2792-2798, doi:10.1016/j.ica.2008.02.002.
55. Morrison, J.S.; Haendler, H.M. Some reactions of tin(II) chloride in nonaqueous solution. *J. Inorg. Nucl. Chem.* **1967**, *29*, 393-400, doi:10.1016/0022-1902(67)80042-3.
56. Sister, M.A.D.; Brother, C.C. Moessbauer and infrared spectra of some tin(II) complexes. *Inorg. Chim. Acta* **1969**, *3*, 169-173, doi:10.1016/S0020-1693(00)92471-X.
57. Bhide, S.N.; Umapathy, P.; Sen, D.N. Oxidative addition reactions of tin(II) oxinates. *J. Indian Chem. Soc.* **1977**, *54*, 851-856.
58. Bhide, S.N.; Umapathy, P.; Gupta, M.P.; Sen, D.N. Tin-119 Moessbauer spectral studies in organotin(IV) and tin(II) substituted oxinates. *J. Inorg. Nucl. Chem.* **1978**, *40*, 1003-1007, doi:10.1016/0022-1902(78)80497-7.
59. Umapathy, P.; Badrinarayanan, S.; Sinha, A.P.B. An ESCA study of tin(IV) and tin(II) chelates with substituted 8-quinolinols. *J. Electron Spectrosc. Relat. Phenom.* **1983**, *28*, 261-266.
60. Uddin, M.J.; Islam, S.; Islam, M.A.; Begum, F.; Haider, S.Z. Synthesis, characterization and antimicrobial properties of some heavy metal oxinates. *J. Bangladesh Chem. Soc.* **1995**, *8*, 7-16.
61. Kitamura, C.; Maeda, N.; Kamada, N.; Ouchi, M.; Yoneda, A. Synthesis of 2-(substituted methyl)quinolin-8-ols and their complexation with Sn(II). *Journal of the Chemical Society, Perkin Transactions 1* **2000**, 781-785, doi:10.1039/a908636f.
62. El-Sonbati, A.Z.; El-Bindary, A.A. Stereochemistry of new nitrogen containing aldehydes. V. Novel synthesis and spectroscopic studies of some quinoline Schiff bases complexes. *Pol. J. Chem.* **2000**, *74*, 621-630.
63. Yoneda, A.; Ohfuchi, S.; Hoshimoto, A.; Kitamura, C. Synthesis and characterization of 2-vinylene-8-quinolinols using the Witting reaction. *Kenkyu Hokoku - Himeji Kogyo Daigaku Kogakubu (Jpn.)* 60-67, *54*, **2002** .

64. Kitamura, C.; Yoneda, A.; Sugiura, K.; Sakata, Y. Bis(2-methyl-8-quinolinolato-N,O)tin(II). *Acta Crystallographica Section C Crystal Structure Communications* **1999**, *55*, 876-878, doi:10.1107/s0108270199002887.
65. Rawson, J.M.; Winpenny, R.E.P. The coordination chemistry of 2-pyridone and its derivatives. *Coordination Chemistry Reviews* **1995**, *139*, 313-374, doi:10.1016/0010-8545(94)01117-t.
66. Parsons, S.; Winpenny, R.E.P. Structural Chemistry of Pyridonate Complexes of Late 3d-Metals. *Accounts of Chemical Research* **1997**, *30*, 89-95, doi:10.1021/ar960162t.
67. Albrecht, M.; Fiege, M.; Osetska, O. 8-Hydroxyquinolines in metallosupramolecular chemistry. *Coordination Chemistry Reviews* **2008**, *252*, 812-824, doi:10.1016/j.ccr.2007.06.003.
68. Dolomanov, O.V.; Bourhis, L.J.; Gildea, R.J.; Howard, J.A.K.; Puschmann, H. OLEX2: a complete structure solution, refinement and analysis program. *Journal of Applied Crystallography* **2009**, *42*, 339-341, doi:10.1107/s0021889808042726.
69. Drover, M.W.; Love, J.A.; Schafer, L.L. 1,3-N,O-Complexes of late transition metals. Ligands with flexible bonding modes and reaction profiles. *Chemical Society Reviews* **2017**, *46*, 2913-2940, doi:10.1039/c6cs00715e.
70. Francis, J.A.; Bott, S.G.; Barron, A.R. Aluminium compounds containing bidentate ligands: chelate ring size and rigid conformation effects. *Journal of the Chemical Society, Dalton Transactions* **1998**, 3305-3310, doi:10.1039/a803667e.
71. Bashall, A.; Beswick, M.A.; Feeder, N.; Hopkins, A.D.; Kidd, S.J.; McPartlin, M.; Raithby, P.R.; Wright, D.S. Reactions of the spiro monoanion [{(Me2N)Sb(μ-NCy)2}2Sb]− with alcohols and thiols (REH; E = O or S); syntheses of nido-[Sb3(μ-NCy)3(μ3-NCy)(ER)2] anions and the unique antimony(III) imido cubane [(2-NC5H4O)Sb(μ3-NCy)]4 (Cy= cyclohexyl). *Journal of the Chemical Society, Dalton Transactions* **2000**, 1841-1847, doi:10.1039/b001322f.
72. Bickley, J.F.; Bond, A.D.; García, F.; Jantos, K.; Lawson, G.T.; McPartlin, M.; Steiner, A.; Wright, D.S. Syntheses and structures of the cubanes [PhOSb(μ3-NCy)]4and [pyOBi(μ3-NCy)]4(Cy = cyclohexyl, py = 2-pyridyl). *J. Chem. Soc., Dalton Trans.* **2002**, 4629-4633, doi:10.1039/b208302g.
73. She, J.-B.; Zhang, G.-F.; Zhao, F.-Q.; Lei, Z.-L.; Fan, X.-Z. The first two structurally characterized energetic catalysts derived from dinitropyridone. *Structural Chemistry* **2007**, *18*, 373-378, doi:10.1007/s11224-007-9179-5.
74. Sunderland, T.L.; Berry, J.F. The first bismuth(II)–rhodium(II) oxypyridinate paddlewheel complexes: synthesis and structural characterization. *Journal of Coordination Chemistry* **2016**, *69*, 1949-1956, doi:10.1080/00958972.2016.1177178.
75. Brewster, T.P.; Nguyen, T.H.; Li, Z.; Eckenhoff, W.T.; Schley, N.D.; DeYonker, N.J. Synthesis and Characterization of Heterobimetallic Iridium–Aluminum and Rhodium–Aluminum Complexes. *Inorganic Chemistry* **2018**, *57*, 1148-1157, doi:10.1021/acs.inorgchem.7b02601.
76. Neufeld, R.; Stalke, D. Accurate molecular weight determination of small molecules via DOSY-NMR by using external calibration curves with normalized diffusion coefficients. *Chemical Science* **2015**, *6*, 3354-3364, doi:10.1039/c5sc00670h.
77. Bachmann, S.; Gernert, B.; Stalke, D. Solution structures of alkali metal cyclopentadienides in THF estimated by ECC-DOSY NMR-spectroscopy (incl. software). *Chemical Communications* **2016**, *52*, 12861-12864, doi:10.1039/c6cc07273a.
78. Kreyenschmidt, A.-K.; Bachmann, S.; Niklas, T.; Stalke, D. Molecular Weight Estimation of Molecules Incorporating Heavier Elements from van-der-Waals Corrected ECC-DOSY. *ChemistrySelect* **2017**, *2*, 6957-6960, doi:10.1002/slct.201701497.
79. Chisholm, M.H.; Clark, D.L.; Hampden-Smith, M.J. Hexaisopropoxyditungsten and dodecaisopropoxytetratungsten: W2(O-i-Pr)6 and W4(O-i-Pr)12. 2. Studies of cluster dynamics and the equilibrium between the 12-electron cluster and two metal-metal triple bonds. A symmetry-allowed [.pi.s2 + .pi.s2] cycloaddition reaction and comparisons with the chemistry of cyclobutadiene. *Journal of the American Chemical Society* **2002**, *111*, 574-586, doi:10.1021/ja00184a027.
80. Boyle, T.J.; Alam, T.M.; Rodriguez, M.A.; Zechmann, C.A. Hydrolysis of Tin(II) Neo-pentoxide: Syntheses, Characterization, and X-ray Structures of [Sn(ONep)2]∞, Sn5(μ3-O)2(μ-ONep)6, and Sn6(μ3-O)4(μ-ONep)4Where ONep = OCH2CMe3. *Inorganic Chemistry* **2002**, *41*, 2574-2582, doi:10.1021/ic011247f.

81. Wang, L.; Kefalidis, C.E.; Sinbandhit, S.; Dorcet, V.; Carpentier, J.-F.; Maron, L.; Sarazin, Y. Heteroleptic Tin(II) Initiators for the Ring-Opening (Co)Polymerization of Lactide and Trimethylene Carbonate: Mechanistic Insights from Experiments and Computations. *Chemistry - A European Journal* **2013**, *19*, 13463-13478, doi:10.1002/chem.201301751.
82. Wiederkehr, J.; Wölper, C.; Schulz, S. Synthesis, solid-state structures and reduction reactions of heteroleptic Ge(II) and Sn(II) β-ketoiminate complexes. *Zeitschrift für Naturforschung B* **2017**, *72*, 813-820, doi:10.1515/znb-2017-0098.
83. Hitchcock, P.B.; Lappert, M.F.; Lawless, G.A.; de Lima, G.M.; Pierssens, L.J.M. Synthesis and structural characterisation of bis(trimethylsilyl)amidotin(II) triflate [{Sn(NR2)-(mu-eta(2)-OTf)(2)}](infinity) (R = SiMe3, -OTf = -OSO2CF3). *Journal of Organometallic Chemistry* **2000**, *601*, 142-146, doi:Doi 10.1016/S0022-328x(00)00048-6.
84. Yao, Z.-F.; Wang, J.-Y.; Pei, J. Control of π–π Stacking via Crystal Engineering in Organic Conjugated Small Molecule Crystals. *Crystal Growth & Design* **2017**, *18*, 7-15, doi:10.1021/acs.cgd.7b01385.
85. Cheng, Y.F.; Emge, T.J.; Brennan, J.G. Pyridineselenolate complexes of tin and lead: Sn(2-SeNC5H4)(2), Sn(2-SeNC5H4)(4), Pb(2-SeNC5H4)(2), and Pb(3-Me(3)Si-2-SeNC5H3)(2). Volatile CVD precursors to group IV group VI semiconductors. *Inorganic Chemistry* **1996**, *35*, 342-346, doi:DOI 10.1021/ic9507326.
86. Dickie, D.A.; Lee, P.T.K.; Labeodan, O.A.; Schatte, G.; Weinberg, N.; Lewis, A.R.; Bernard, G.M.; Wasylishen, R.E.; Clyburne, J.A.C. Flexible coordination of the carboxylate ligand in tin(ii) amides and a 1,3-diaza-2,4-distannacyclobutanediyl. *Dalton Transactions* **2007**, doi:10.1039/b704588c.
87. Wächtler, E.; Gericke, R.; Kutter, S.; Brendler, E.; Wagler, J. Molecular structures of pyridinethiolato complexes of Sn(II), Sn(IV), Ge(IV), and Si(IV). *Main Group Metal Chemistry* **2013**, *36*, doi:10.1515/mgmc-2013-0041.
88. Barbul, I.; Johnson, A.L.; Kociok-Köhn, G.; Molloy, K.C.; Silvestru, C.; Sudlow, A.L. The Reaction and Materials Chemistry of [Sn6(O)4(OSiMe3)4]: Chemical Vapour Deposition of Tin Oxide. *ChemPlusChem* **2013**, *78*, 866-874, doi:10.1002/cplu.201300104.
89. Schiemenz, B.; Ettel, F.; Huttner, G.; Zsolnai, L. Metallorganische schutzgruppen für den aufbau ungewöhnlicher zinn-chalkogen-käfigverbindungen: Thiostannat(II) Sn3S42− und "Zinnoxidhydrat" Sn6(μ3-OH)4(μ3-O)4 als Liganden in RCp(CO)2Mn-Komplexen. *Journal of Organometallic Chemistry* **1993**, *458*, 159-166, doi:10.1016/0022-328x(93)80468-q.
90. Sita, L.R.; Xi, R.; Yap, G.P.A.; Liable-Sands, L.M.; Rheingold, A.L. High Yield Synthesis and Characterization of Sn6(μ3-O)4(μ3-OSiMe3)4: A Novel Main Group Cluster for the Support of Multiple Transition Metal Centers. *Journal of the American Chemical Society* **1997**, *119*, 756-760, doi:10.1021/ja963450t.
91. Kircher, P.; Huttner, G.; Zsolnai, L.; Driess, A. Partially Oxidized Zintl Ions? The Characterization of [(μ3-OH)(μ3-O)3(OEt)3{(CO)5W}7Sn7]2−. *Angewandte Chemie International Edition* **1998**, *37*, 1666-1668, doi:10.1002/(sici)1521-3773(19980703)37:12<1666::Aid-anie1666>3.0.Co;2-v.
92. Mertens, L.; Leonhardt, C.; Rüffer, T.; Toma, A.; Silvestru, C.; Mehring, M. Heterobimetallic tin(II) oxido clusters of the type [{Sn 6 (μ 3 -O) 4 (μ 3 -OCH 2 R) 4 } {W(CO) 5 } 4] and [{Sn 5 (μ 3 -O) 2 (μ-OCH 2 R) 4 (μ 3 -OCH 2 R) 2 }{Fe(CO) 4 } 2]. *Journal of Organometallic Chemistry* **2016**, *821*, 206-213, doi:10.1016/j.jorganchem.2016.04.026.
93. Freidzon, A.Y.; Safonov, A.A.; Bagaturyants, A.A. Theoretical Study of the Spectral and Charge-Transport Parameters of an Electron-Transporting Material Bis(10-hydroxybenzo[h]qinolinato)beryllium (Bebq2). *The Journal of Physical Chemistry C* **2015**, *119*, 26817-26827, doi:10.1021/acs.jpcc.5b08239.
94. Wu, X.S.; Sun, H.S.; Pan, Y.; Chen, H.B.; Sun, X.Z. The reaction of metal trialkyls with benzo[H]quinolin-10-ol. *Chin. Chem. Lett.* **1999**, *10*, 875-878.
95. Fjeldberg, T.; Hope, H.k.; Lappert, M.F.; Power, P.P.; Thorne, A.J. Molecular structures of the main group 4 metal(II) bis(trimethylsilyl)-amides M[N(SiMe3)2]2 in the crystal (X-ray) and vapour (gas-phase electron diffraction). *Journal of the Chemical Society, Chemical Communications* **1983**, doi:10.1039/c39830000639.